Research Article
High-Performance Emulator for Fixed Photovoltaic Panels

Youssef Mallal [ID]**, Lhoussain El Bahir** [ID]**, and Touria Hassboun** [ID]

Laboratory of Electrical Engineering and Control Systems (LGECOS), National School of Applied Sciences, Cadi Ayyad University, Av. Abdelkrim El Khattabi B.P. 575, 40000 Marrakech, Morocco

Correspondence should be addressed to Youssef Mallal; mallalyoussef52@gmail.com

This paper presents the design and implementation of a photovoltaic emulator, based on an accurate mathematical model of a photovoltaic panel, instead of the look-up table method. The latter requires more memory for increasing accuracy and considering all the desired environmental situations. Furthermore, the proposed approach takes into account the incidence solar angle, as an input parameter, to offer the possibility of evaluating daily losses for different values of tilt angle. The validation of the proposed emulator is carried out by comparing in real-time, both the studied panel output and the emulator output, under variable load, temperature, and irradiation levels. The emulator is able to operate online with connected solar radiation and temperature sensors or offline with recorded measurement vectors. The practical tests were performed on a prototype designed using a MATLAB C MEX S-function, dSPACE board 1104, and a controlled DC/DC converter. The results showed that the emulator was able to behave accurately as the studied photovoltaic panel.

1. Introduction

Photovoltaic emulators are nowadays becoming an alternative solution for indoor studying and analysing of photovoltaic systems. Recall that, those electronic power devices are able to reproduce the electrical behaviour of photovoltaic panels under controllable conditions.

In the literature, several methods to emulate photovoltaic panel behaviour have been studied. The reference generation could be analogue or digital; in [1, 2], two analogue reference generations were presented. The photovoltaic emulator developed in [1] consists in amplifying a photodiode I-V characteristic, which is considered as a PV cell. This method needs a light-emitting diode to simulate solar irradiation. Temperature control is ensured by a temperature controller of the photodiode. The authors in [2] have proposed a method to emulate the photovoltaic panel behaviour based on a logarithmic amplifier, operational amplifiers, variable resistors, adjustable linear voltage regulator, and a DC power supply. Although the analogue methods do not have a calculation delay, they are not flexible when controlling temperature and irradiation levels. An alternative solution is using digital reference generation combined with a power con-

verter. In the literature review, different digital controllers were used, namely, the microcontroller [3], the field-programmable gate array (FPGA) [4], and the digital signal processor (DSP) [5]. A hybrid digital-analogue reference generation is presented in [6].

A photovoltaic emulator can be considered as a controlled DC power supply able to reproduce photovoltaic panel characteristics, regardless of the environmental conditions. The general architecture of the PV emulator is shown in Figure 1.

It consists of three main elements: PV model implementation, control strategy, and power stage control [7]. The PV model reproduces the photovoltaic panel characteristic to be emulated; it receives as inputs, the temperature and the radiation in addition to measured photovoltaic panel voltage or current, according to the control type used for the power converter, current controlled or voltage controlled. The control strategy is the stage between the PV model and the power converter. It determines the intersection point between the photovoltaic emulator characteristic and the load characteristic. The power converter could be a linear regulator, a switching mode power supply, or a programmable DC power supply including the closed-loop control. The switching
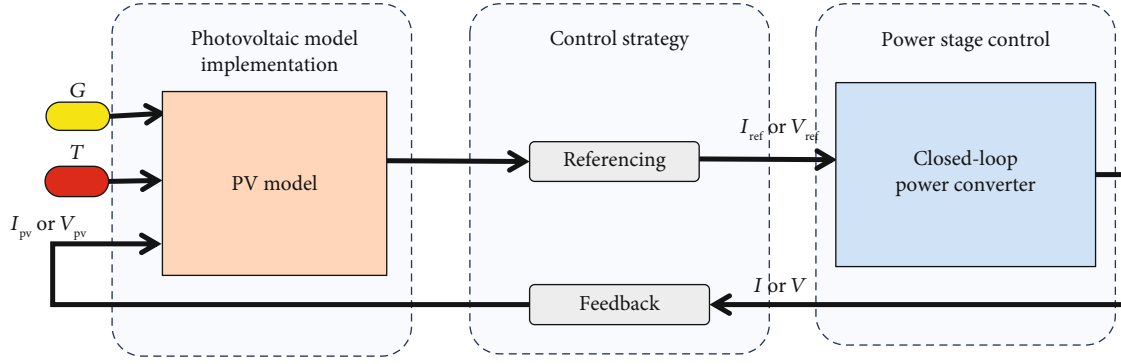
FIGURE 1: General photovoltaic emulator architecture.

mode power supplies are recommended for high-power applications, due to their efficiency and fast dynamic response.

Despite all the studies carried out for the design and implementation of photovoltaic emulators, the existing structures do not take into account all the operating conditions of solar panels, such as the geographical position, time, tilt angle of photovoltaic panels, and wind effect.

In this paper, we propose a new architecture of the photovoltaic emulator able to study the electrical characteristics of fixed photovoltaic installations, by considering time, tilt angle, latitude, and longitude as additional input parameters. The proposed emulator can also be used for loss estimation or tilt angle optimization. The control algorithm is implemented using a flexible direct calculation method to cover all temperature and irradiation levels. The design and the implementation are carried out on the dSPACE 1104 controller board. The DC/DC converter is designed to support the current delivered by the SR-20 panel under different operating conditions. One of the strong points of the proposed emulator is the ability to reproduce, in real-time, a very accurate electrical power, synchronously with a reference PV panel under real weather conditions and variable load. The results showed a good agreement between the emulator and the panel responses in transient and steady states.

The rest of the paper is organized as follows. The proposed emulator implementation is given in Section 2; the model of the photovoltaic panel and its practical validation are presented in Section 3. Section 4 is dedicated to the design and control strategy of the power converter. Section 5 presents real-time implementation results and analysis. Finally, some concluding remarks and perspectives are presented in the last section.

2. Structure of the Proposed Photovoltaic Emulator

Photovoltaic emulators developed in the literature emulate the photovoltaic panel behaviour at the desired temperature and solar irradiation. The latter is influenced by the incidence angle of the sunrays, which represents the angle between the sunlight and the normal to the surface of the panel. The reflected and diffuse solar radiations can be neglected compared to the direct solar radiation G_D. The effective solar radiation G_i received by the panel for a given incidence angle i, is given by [8]:

$$G_i = \cos(i) \times G_D. \tag{1}$$

The incidence angle of solar radiation on an inclined panel depends on several angles. The illustration of these angles is presented in Figure 2, where BO is the normal to the horizontal surface, CO is the normal to the tilt surface, OE is the projection of the normal to the inclined surface on the horizontal plane, γ is the surface azimuth angle, and β is the tilt angle, measured from the horizontal. By applying cosine law on various mentioned above angles, one can deduce the following relationships [9]:

$$\cos(i) = \cos(\beta)\cos(z) + \sin(\beta)\sin(z)\cos(\alpha - \gamma),$$
$$\sin(\alpha) = \frac{\sin(\omega)\cos(\delta)}{\sin(z)},$$
$$\cos(z) = \sin(\delta)\sin(\phi) + \cos(\delta)\cos(\phi)\cos(\omega),$$
$$\delta = 23.45° \sin\left[\frac{360}{365}(284 + d)\right],$$
$$\omega = (ST - 12) \times 15°,$$
$$ST = t + ET \pm 4(L_{ST} - L) + DST,$$
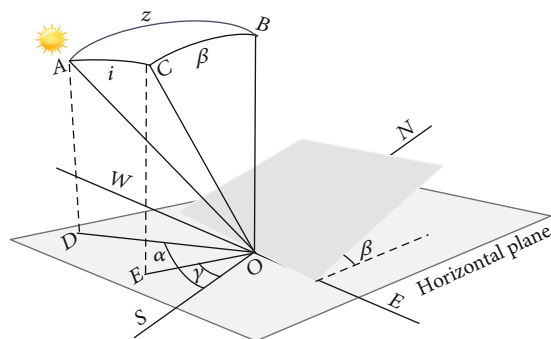$$L_{ST} = 15°\Delta GMT,$$
$$ET = 229.2(0.000075 + 0.001868\cos(B)$$
$$- 0.032077\sin(B) - 0.014615\cos(2B)$$
$$- 0.04089\sin(2B)),$$
$$B = (d - 1)\frac{360}{365},$$

$$\tag{2}$$

where z is the zenith angle, ϕ is the latitude, α is the solar azimuth angle, δ is the declination angle, d is the day of the year, ω is the solar hour angle, ST is the solar time, L_{ST} is the local standard time meridian, LT is the local time, GMT is the Greenwich Mean Time, in hours, ΔGMT is the difference of

FIGURE 2: Solar radiation on tilt photovoltaic panel.

LT and GMT, L is the longitude, ET is the equation time, DST is the daylight saving time, and t is the standard time.

The incidence angle in terms of declination angle, tilt angle, latitude, and hour angle is given by:

$$\cos (i) = \sin (\delta)[\sin (\phi) \cos (\beta) - \cos (\phi) \sin (\beta)] \\ + \cos (\delta) \cos (\omega)[\cos (\phi) \cos (\beta) \\ + \sin (\phi) \sin (\beta) \cos (\gamma)]. \tag{3}$$

When the inclined photovoltaic panel faces the equator ($\gamma = 0$), equation (3) becomes

$$\cos (i) = \sin (\delta)[\sin (\phi) \cos (\beta) - \cos (\phi) \sin (\beta)] \\ + \cos (\delta) \cos (\omega)[\cos (\phi) \cos (\beta) + \sin (\phi) \sin (\beta)]. \tag{4}$$

Hence,

$$\cos (i) = \sin (\phi - \beta) \sin (\delta) + \cos (\phi - \beta) \cos (\delta) \cos (\omega). \tag{5}$$

The developed emulator architecture is shown in Figure 3.

According to equation (1), the cosine of the incidence angle is multiplied by the solar radiation to calculate the actual value of solar radiation received by the panel, under the installation conditions. From the user-defined inputs and the measured voltage V_{pve}, considered as the emulator voltage, the PV model generates a current reference I_{ref} that will be compared with the current-controlled buck converter output I_{pve}, considered as the emulator current. The error is minimized by the PI controller to maintain I_{pve} to its reference value I_{ref}. The model and control algorithm are programmed under MATLAB/Simulink and loaded on the dSPACE controller board. The LEM LA55-P and the LEM LV20-P are, respectively, the current and the voltage sensors. Their outputs are connected to a conditioning circuit to deliver a voltage between 0 and ±10 volts, adapted as an input of the dSPACE board ADC.
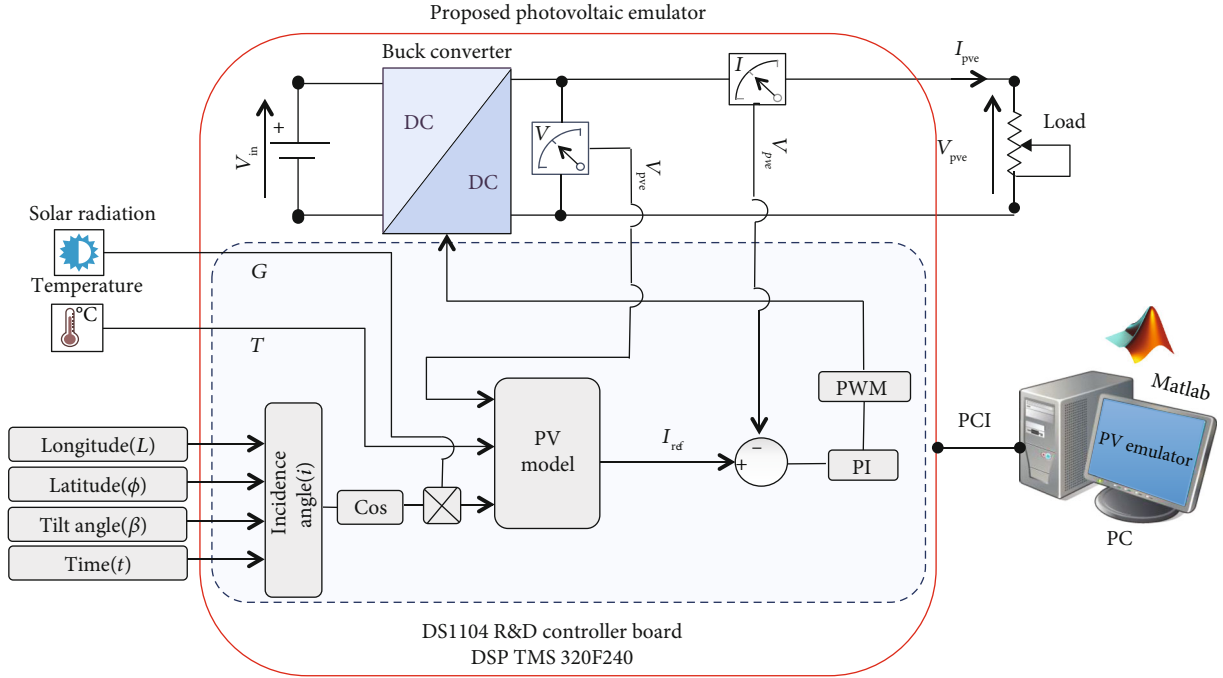
The dSPACE board contains a Master Floating-Point DSP (400 MHz) for processing and a Slave DSP (20 MHz) for controlling PWM and digital I/Os. The control parameters, the sensor gains, and the data visualization are carried out under ControlDesk software.

The major targeted goals, during the development of this architecture, are (i) the design of a photovoltaic emulator with the same response as a photovoltaic panel in the transient and steady state, (ii) considering the actual installation conditions of photovoltaic panels. (iii) The emulator must be able to operate in real-time with connected temperature and radiation sensors or with stored data from other stations, (iv) a simple and accurate control law easy to be implemented in other platforms. The details of the implementation and design of each part of the architecture are given in the following sections.

3. Photovoltaic Panel Model Implementation

A photovoltaic cell is an electric power generator, consisting of semiconductor layers that convert solar energy into electricity. Depending on the load connected to its terminals, it can behave as a current source or as a voltage source [10]. In the literature review, several photovoltaic models are used to simulate the photovoltaic panel behaviour. They are divided into two categories: electrical circuit models based on the electrical characteristics of the photovoltaic panel and interpolation models based on the IV characteristic of the photovoltaic panel [11]. Even if the electrical circuit models are less fast compared with the linear models, they are commonly used by the researchers, due to their accuracy. The most popular electric models are the double diode model and the single diode model. The latest presents a good compromise between accuracy and simplicity [12]. The photovoltaic model implementation is carried out by several methods, direct calculation method, look-up table method, piecewise-linear method, neural network method, and photovoltaic elimination voltage method [7]. The direct calculation method is characterized by good accuracy and low memory demand. In this paper, we used an electric model (1D2R) with a numerical calculation method to avoid the use of look-up tables to increase the model accuracy. The 1D2R model with the equivalent circuit is shown in Figure 4.

The current-voltage characteristic of a photovoltaic module is represented by equation (8).

$$I = I_{\mathrm{ph}} - I_D - I_p, \tag{6}$$

where

$$I_D = I_0 \left(e^{V/AV_t} - 1 \right), \\ I_p = \frac{V + R_s I}{R_p}. \tag{7}$$

Figure 3: Proposed photovoltaic emulator architecture.
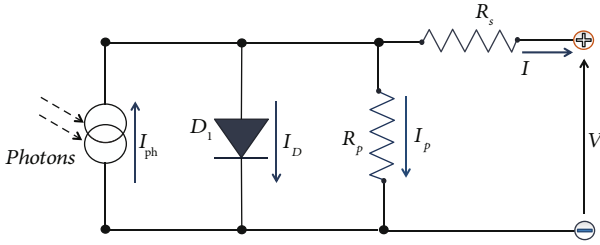

Figure 4: Equivalent circuit model of the 1D2R model.

Hence,

$$I = I_{\text{ph}} - I_0 \left(e^{((V+R_sI)/V_tA)} - 1 \right) - \frac{V + R_sI}{R_p}. \tag{8}$$

The current I_{ph} describes the photogenerated current of the photovoltaic panel; it depends on solar radiation and temperature as follows:

$$I_{\text{ph}} = \frac{G}{G_n} [I_{\text{scr}} + K_i(T - T_r)]. \tag{9}$$

$V_t = kTc/q$ is the thermal voltage, k is the Boltzmann constant, T is the temperature of the photovoltaic panel and A is the diode ideality factor, q is the electronic charge, T_r is the reference temperature, I_{scr} is the short circuit current at T_r, K_i is the short circuit current/temperature coefficient, and G_n is the nominal irradiation.

The reverse saturation current of diode I_0 may be expressed by

$$I_0 = I_n \left(\frac{T_c}{T_r} \right)^3 e^{\left(qE_g/Ak \right)((1/T_r)-(1/T_c))}, \tag{10}$$

where I_n is the nominal saturation current and E_g is the band gap energy.

The identification of the unknown parameters mentioned above is based on the physical parameters of the studied panel, given in the manufacturer's datasheet at standard test conditions (STCs) of temperature and solar irradiation. The specifications of the SR-20 panel are given in Table 1.

The model is programmed as a C MEX S-Function and loaded on the dSPACE 1104 controller board. Firstly, the model is validated in simulation as shown in Figure 5.

As can be seen in Figure 5, the simulated current-voltage and power-voltage characteristics, under nominal conditions of temperature and irradiation, reproduce the same values of V_{OC}, I_{SC}, V_{MP}, and I_{MP}. The model is also validated with real data of irradiation and temperature recorded for short cloudy periods. The results of this validation have shown that the model behaves exactly as the SR-20 panel, under variable conditions of temperature and irradiation, as shown in Figure 6.

4. Power Stage Design and Control

There are three main power converters used in photovoltaic emulator applications: linear regulator [1], programmable DC power supply [13], and Switching-Mode Power Supply

TABLE 1: SR-20 PV panel specifications (A.M.1.5, $1\,kW/m^2$, 25°C) and identified parameters of the adjusted model.

Voltage at MPP (V_{MP})	17.2 V
Current at MPP (I_{MP})	1.17 A
Short circuit current (I_{SC})	1.28 A
Open circuit voltage (V_{OC})	21.6 V
Maximum power (P_{MP})	20 W
Ideality factor (A)	1.9
Charge of electron (q)	1.6e-19 C
Boltzmann constant (k)	1.38e-23 J/K
Band gap energy (E_g)	1.12 eV
Reverse saturation current at T_r (I_n)	5.98e-6 A
Temperature coefficient of SC current (K_i)	512.10-6 A/K
Number of cells connected in series (n_s)	36
Number of cells connected in parallel (n_p)	1
Internal series resistance of a cell (R_s)	0.004 Ω
Internal parallel resistance of a cell (R_p)	1000 Ω

FIGURE 6: Model validation under natural conditions.

FIGURE 5: I-V and P-V characteristics of the PV panel at $1000\,W/m^2$, $T = 25$°C.

(SMPS) [4]. Since the efficiency of the linear regulator is low, it is rarely used in photovoltaic emulator applications. The programmable DC power supply includes the closed-loop control, but it suffers from the response delay. As a result, the SMPS is more suitable for photovoltaic emulators in terms of efficiency and dynamic response. Among the common SMPS topologies, a buck converter is used to cover the values of the emulated panel I-V characteristic. The control type is current control, ensured by a PI controller. The electrical circuit of the buck converter is shown in Figure 7, operating in the continuous conduction mode (CCM). The design parameters are given in Table 2.

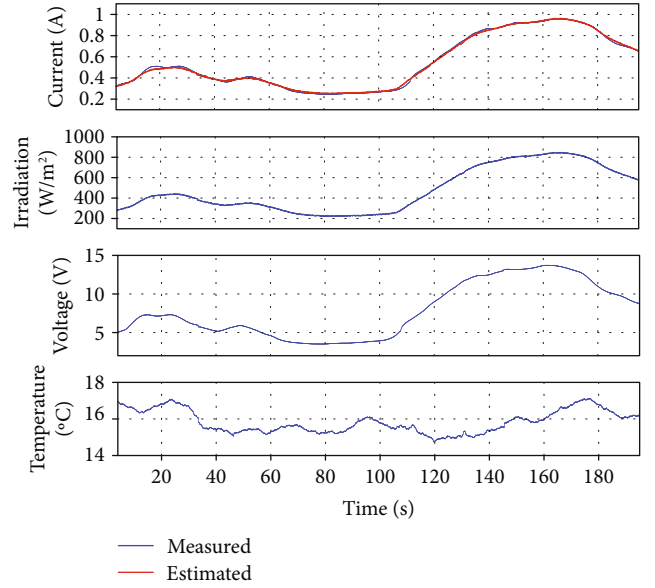The selection of the values of C and L is based on the standard design equations. The DC-DC buck converter was

built using IRF540NPBF MOSFET connected to FOD3120 gate driver. The selected values of L and C are 1 mH and 470 μF, respectively.

The closed-loop control is shown in Figure 8. It consists of a PI controller receiving the current reference from the PV model. The buck converter is current-controlled. Its transfer function, derived from the small-signal analysis, is given by [7]:

$$G_{BUCK}(s) = \frac{\hat{i}_{pve}(s)}{\hat{d}(s)} = \frac{V_{in}/R}{LCs^2 + (L/R)s + 1}. \quad (11)$$

The second-order term coefficient, LC, could be neglected ($LC \sim 1e\text{-}7$) compared to L/R ($L/R \sim 1e\text{-}3$). The system can then be considered as a first-order system, equation (22).

$$G_{BUCK}(s) = \frac{\hat{i}_{pve}(s)}{\hat{d}(s)} = \frac{V_{in}/R}{(L/R)s + 1}. \quad (12)$$

The PI parameters are tuned to ensure a fast response, stability, and minimizing steady-state error. The closed-loop responses for abrupt load and setpoint changes are given in Figure 9. As can be seen, the designed controller is able to track the setpoint I_{ref} regardless of load and reference change conditions.

As mentioned previously, the control strategy plays a very important role in the determination of the operating point. There are several control strategies of photovoltaic emulators reported in the literature, namely, the resistance comparison method [14], the hill-climbing method [15], the hybrid-mode controlled method [16], and the direct referencing method [7]. In this study, we used a direct referencing method that works with the SMPS and does not
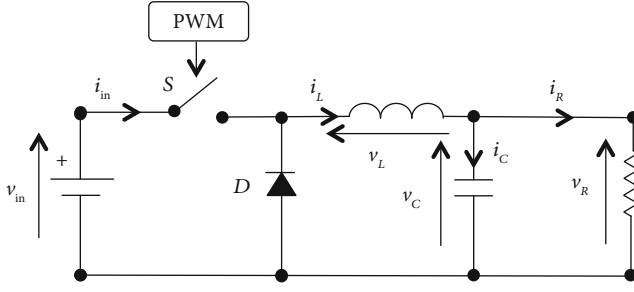
Figure 7: Buck converter architecture.

Table 2: Design parameters of buck converter.

Input voltage (V_{in})	24 V
Switching frequency (f_{SW})	20 kHz
Output voltage ripple (ΔV)	10 mV
Inductor current ripple (ΔI)	30%

require any additional algorithm. This method involves connecting the emulator output voltage V_{pve} to the PV model input. The latter generates a current reference I_{ref} applied to the PI controller input, Figure 8.

At the start time, the $V_{pve} = 0$ and the photovoltaic model generates a reference current $I_{ref} = I_{sc}$, for a given load, irradiance, and temperature. As V_{pve} increases, I_{ref} begins to decrease following the PV panel I-V characteristic. The PV emulator stabilizes on an operating point when V_{pve} and the output current I_{pve}, correspond to the output resistance R_{Load} on the I-V characteristic, Figure 10.

5. Results and Discussion

Unlike previous works in this domain, the superiority of the method in real-time processing was experimentally validated by connecting the photovoltaic panel and the emulator to two similar resistive loads and comparing simultaneously both panel and emulator outputs. Under the same variable conditions of temperature, solar radiation, load, latitude, longitude, time, and tilt angle, the emulator must be able to deliver the same voltage and current as the SR-20 solar panel. The scheme of the practical platform is illustrated in Figure 11.

A photograph of the experimental platform, with its instrumentation, is shown in Figure 12. The solar radiation, current, voltage, and temperature are, respectively, measured by CM10, LEM LA55-P, LEM LV20-P, and PT1000 sensors. The signals pass through a conditioning circuit to deliver voltages between 0 and ± 10 volts, adapted to ADC inputs of the dSPACE controller board. The photovoltaic emulator was tested under variable load, solar radiation, and temperature. The validation results are given in the next subsections.

Experimental tests were carried out during alternating sunny and cloudy periods, in Marrakech on April 2nd,

2019, from 14 h 30 mins to 17 h 30 mins. The SR-20 panel is fixed in a position of 31 degrees facing south. The validation was carried out progressively, by first individually testing the effect of each of the factors, including load, irradiation, and temperature and secondly the simultaneous variation of the different factors, taking into account the effect of the solar incidence angle studied in Section 2.

5.1. Electrical Characteristic Verification. To demonstrate the validity of the proposed emulator, it would be appropriate to start with standard offline tests, based on controlled G and T variations. To generate the I-V characteristics, the proposed emulator was connected to a variable load, for different values of solar radiation and temperature. The comparison between the obtained I-V characteristics and those of the reference panel is given in Figure 13. Test results have shown that the proposed emulator behaves exactly like the SR-20 panel, throughout the I-V characteristic.

Since the incidence angle is related to real-time operation of the PV system, the integration of its effect on the emulator is validated subsequently.

5.2. Load Variation. When changing the load, the emulator and the photovoltaic panel are each connected to three resistive loads (19 Ω, 15 Ω, and 9 Ω); switching from one load to another is carried out, simultaneously, by controlled relays. Figure 14 illustrates the behaviour of the emulator and panel under load variation and during a period when the temperature and irradiation are considered constant. As can be seen from the curve, the emulator faithfully reproduces the same electrical behaviour as the SR-20 panel.

5.3. Irradiation Variation. The effect of variable irradiation at stable temperature (at 29°C) is shown in Figure 15. The tests are performed under periods of dense and less dense clouds, inducing a variation of solar irradiation between 375 W/m² and 627 W/m². The results showed that the emulator was able to follow accurately abrupt changes in irradiation with a high robustness degree.

5.4. Simultaneous Variation of Load and Environmental Conditions. In natural operation, photovoltaic panels work under uncontrollable environmental and load conditions. A powerful emulator should be able to reproduce the same electrical behaviour as a photovoltaic panel under such conditions. The test conditions are shown in Figure 16. As can be seen, the emulator behaves in a very efficient way throughout the test, in particular, the area between 15 and 25 mins where the three factors vary at the same time.

5.5. Incidence Angle Effect. To study the electrical behaviour of a fixed installation through an emulator, it would be appropriate to consider the incidence angle effect on the electrical photovoltaic panel characteristic. In about 20 mins, between 14 h 30 mins and 14 h 50 mins, the incidence angle presents a variation of more than 3 degrees, leading to a progressive output emulator error. At 14 h 50 mins, an adjustment of the incidence angle was introduced in the emulator input, as shown in Figure 17.
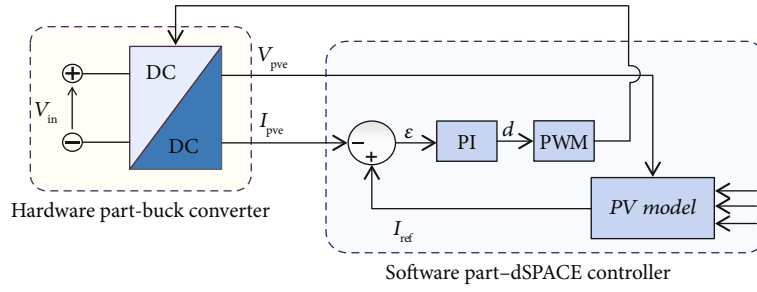
FIGURE 8: Power stage closed-loop control.
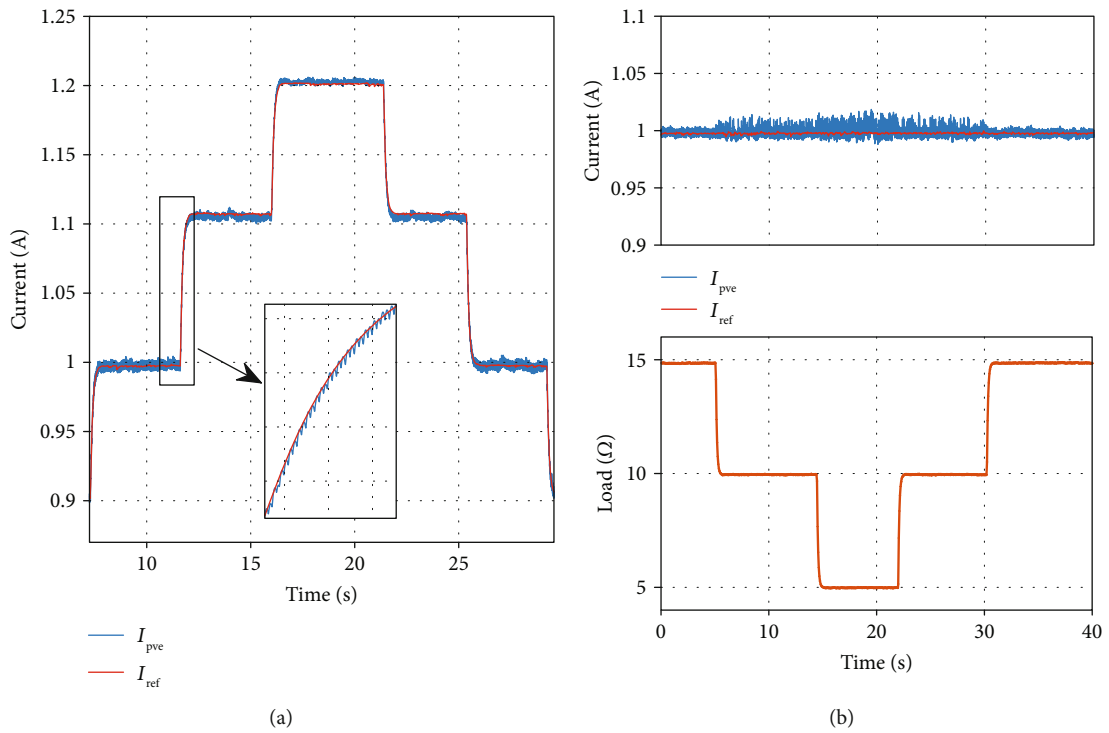

(a)

(b)

FIGURE 9: (a) Closed-loop response for abrupt setpoint change, (b) closed-loop response for abrupt load change.
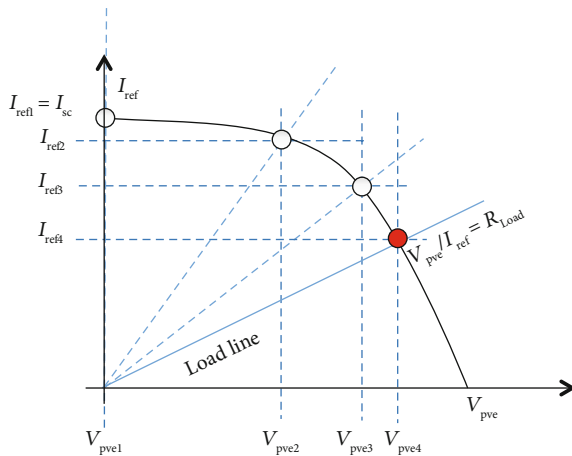

FIGURE 10: Control strategy principle.

An overall summary test was performed in real-time on a fixed panel for 2 h 30 mins, to highlight the performance of our emulator for the final prototype, Figure 18. During the test, the solar irradiation and the temperature show significant natural variations. The load varies arbitrarily between $19\,\Omega$, $15\,\Omega$, and $9\,\Omega$. The emulator combines the measured solar irradiation with an estimated incidence angle to determine the actual irradiation received by the panel. The incidence angle changes from 49° to 82°. The current and the voltage generated by the emulator, under the same conditions, show a perfect agreement with those delivered by the photovoltaic panel under consideration.

6. Conclusion

In this paper, a prototype of a high-performance photovoltaic emulator has been developed, including the effect
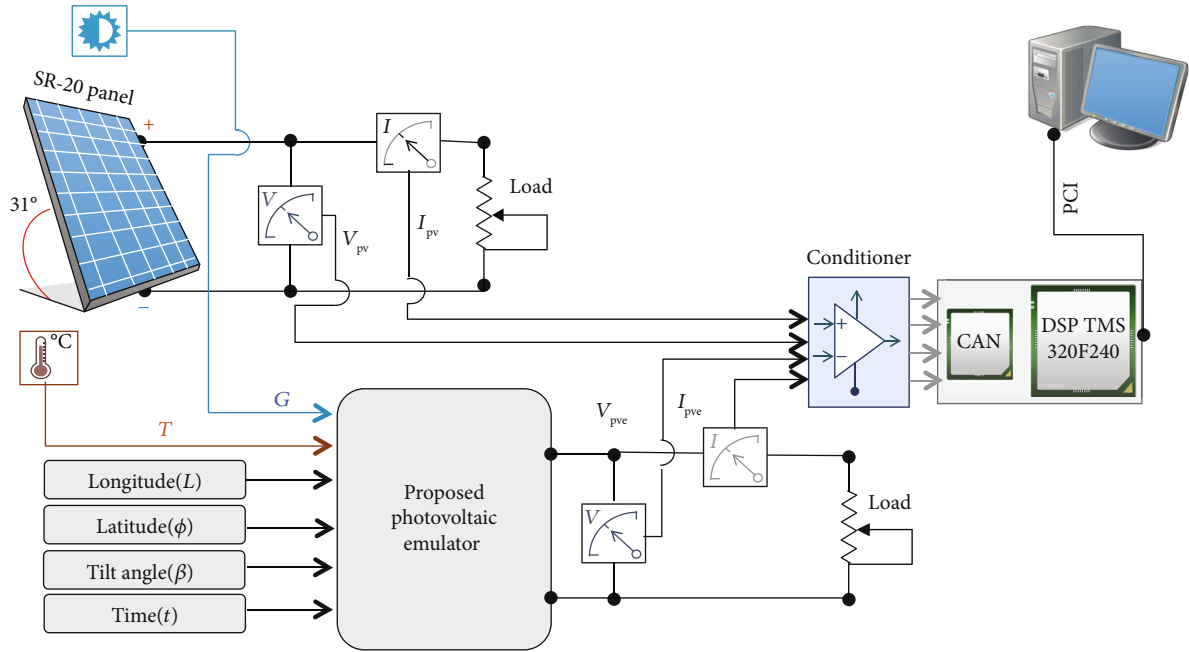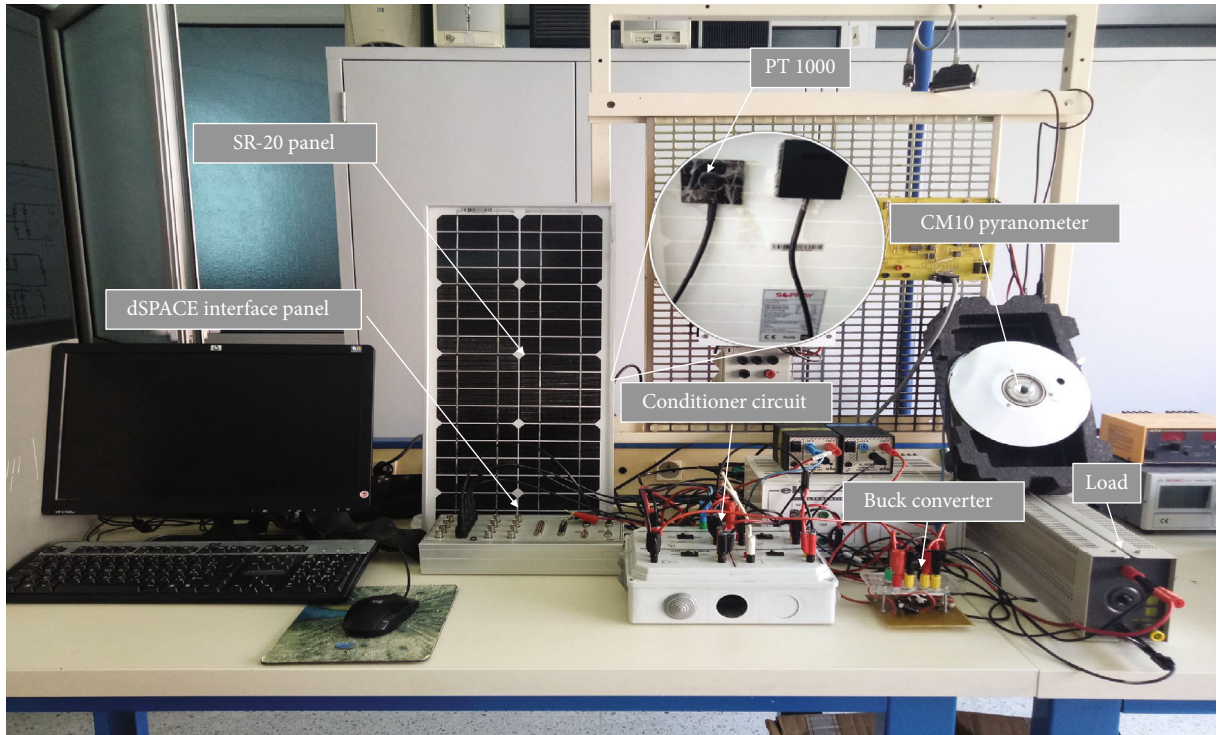
FIGURE 11: Experimental validation scheme.

FIGURE 12: A photograph of the experimental platform.

of the incidence angle. The experimental validation was carried out in real-time, by comparing both panel and emulator outputs.

As the converter is a key element in the emulator architecture, special attention has been given to its control system

to maintain the same performance for any operating point. The proposed control algorithm is based on an autotuning PI controller, according to load and input voltage variations. The method leads to a simple and accurate control law easy to implement on any digital platform.
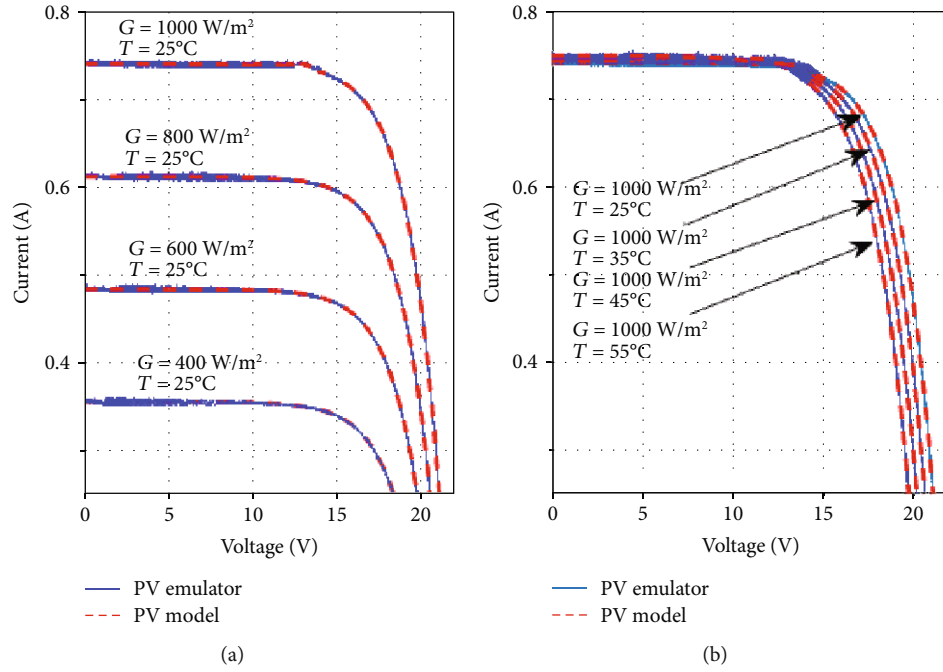
(a)

(b)

FIGURE 13: (a) Generated I-V characteristics for a fixed temperature and variable solar radiation, (b) generated I-V characteristics for a variable temperature and fixed solar radiation.
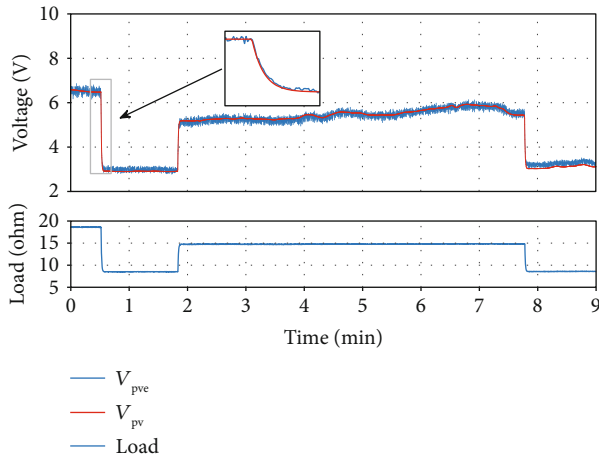

FIGURE 14: Proposed emulator test under load variation.
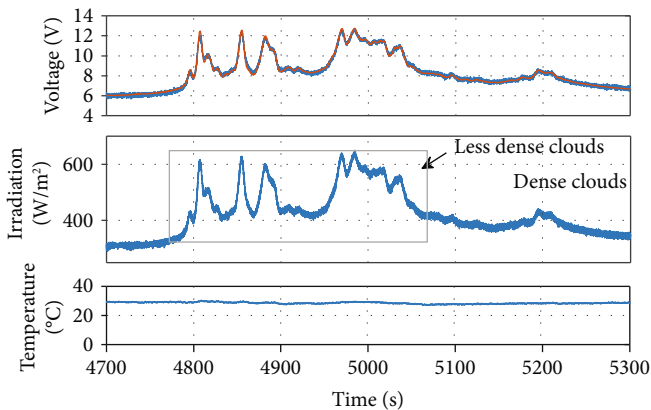

FIGURE 15: Proposed emulator test under variable irradiation.
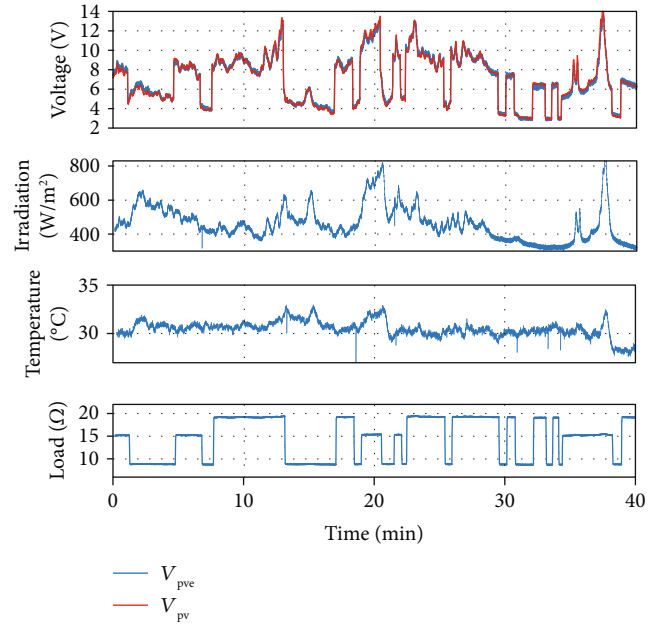

FIGURE 16: Proposed emulator test under simultaneous variation of load and environmental conditions.

To validate all expected performances of the proposed emulator structure, a practical platform has been designed and developed for this purpose. A global test scenario was used to validate the dynamic and steady-state responses of the emulator under realistic and possible operating conditions.
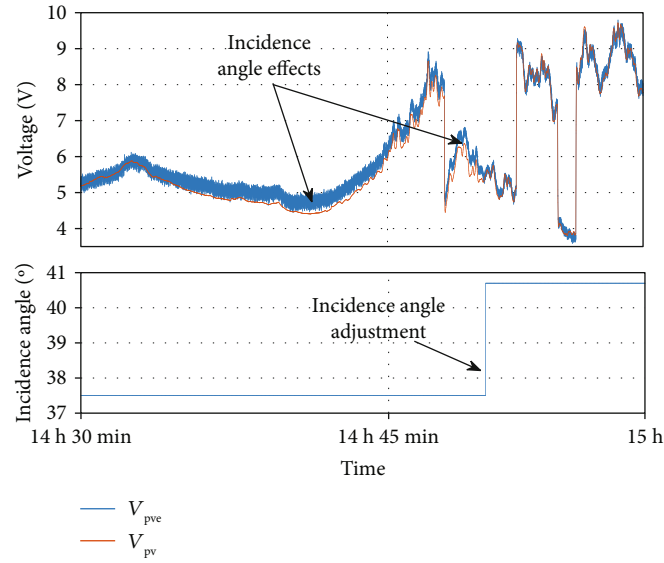
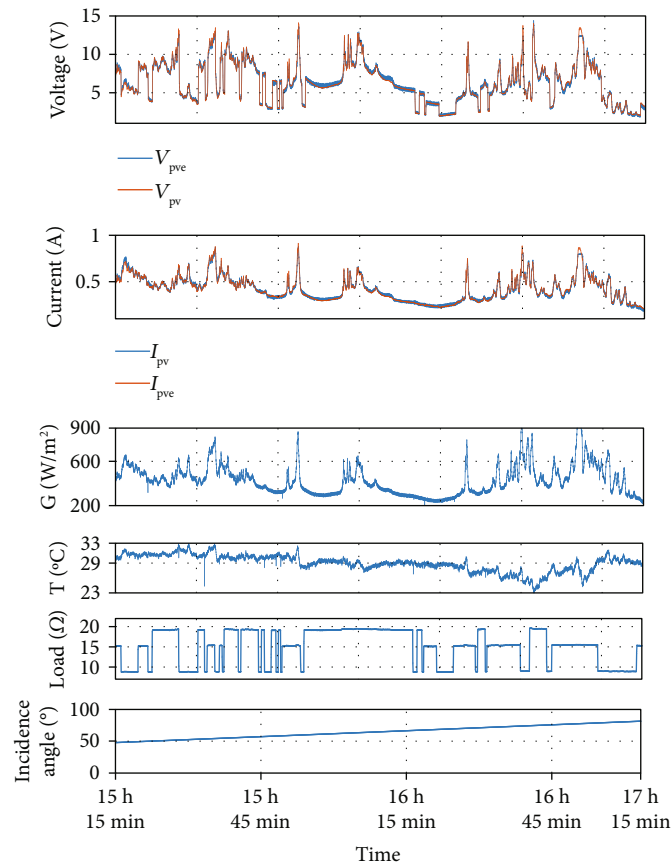FIGURE 17: Incidence angle effect on emulator output.

FIGURE 18: Proposed emulator test under real use conditions with automatic incidence angle adjusting.

The obtained results showed that the emulator could behave accurately as the reference photovoltaic panel under variable environmental conditions and load abrupt changes. The results showed also that for a fixed panel the emulator considers efficiently the daily incidence angle evolution.

A hardware platform based on a low-cost digital controller is under development.

Data Availability

The data used to support the findings of this study are available from the corresponding author upon request.

Conflicts of Interest

The authors declare that they have no conflicts of interest.

References

[1] I. Moussa, A. Khedher, and A. Bouallegue, "Design of a low-cost PV emulator applied for PVECS," *Electronics*, vol. 8, no. 2, p. 232, 2019.

[2] H. Nagayoshi, "*I–V* curve simulation by multi-module simulator using *I–V* magnifier circuit," *Solar Energy Materials and Solar Cells*, vol. 82, no. 1-2, pp. 159–167, 2004.

[3] C. Balakishan and S. Babu, "Development of a microcontroller based PV emulator with current controlled DC/DC buck converter," *International Journal of Renewable Energy Research*, vol. 4, no. 4, pp. 1049–1055, 2014.

[4] D. Ickilli, H. Can, and K. S. Parlak, "Development of a FPGA-based photovoltaic panel emulator based on a DC/DC converter," in *2012 38th IEEE Photovoltaic Specialists*, pp. 001417–001421, Austin, TX, USA, 2012.

[5] P. H. To and D. Q. Phan, "A photovoltaic emulator using dSPACE controller with simple control method and fast response time," in *2017 International Conference on System Science and Engineering (ICSSE)*, pp. 718–723, Ho Chi Minh City, Vietnam, 2017.

[6] G. Vachtsevanos and K. Kalaitzakis, "A hybrid photovoltaic simulator for utility interactive studies," *IEEE Transactions on Energy Conversion*, vol. EC-2, no. 2, pp. 227–231, 1987.

[7] R. Ayop and C. W. Tan, "A comprehensive review on photovoltaic emulator," *Renewable and Sustainable Energy Reviews*, vol. 80, pp. 430–452, 2017.

[8] M. A. Ionita and C. Alexandru, "Simulation of a dual-axis tracking system for PV modules," *Bulletin of the Transilvania University of Brasov Engineering Sciences Series I*, vol. 4, no. 2, p. 45, 2011.

[9] J. E. Braun and J. C. Mitchell, "Solar geometry for fixed and tracking surfaces," *Solar Energy*, vol. 31, no. 5, pp. 439–444, 1983.

[10] T. Hassboun, L. El Bahir, Y. A. DRISS, and M. El Adnani, "Solar irradiation estimator based on a self-calibrated reference solar cell," *Turkish Journal of Electrical Engineering & Computer Sciences*, vol. 24, no. 6, pp. 4885–4899, 2016.

[11] R. Ayop and C. W. Tan, "A comparison study of interpolation and circuit based photovoltaic mathematical models," in *2016 IEEE International Conference on Power and Energy (PECon)*, pp. 626–631, Melaka, Malaysia, 2016.

[12] L. E. Bahir and T. Hassboun, "Accurate maximum power point tracking algorithm based on a photovoltaic device model," *International Journal of Photoenergy*, vol. 2017, Article ID 5693941, 10 pages, 2017.

[13] A. F. Ebrahim, S. M. W. Ahmed, S. E. Elmasry, and O. A. Mohammed, "Implementation of a PV emulator using programmable DC power supply," in *SoutheastCon 2015*, pp. 1–7, Fort Lauderdale, FL, USA, 2015.

[14] R. Ayop and C. W. Tan, "Improved control strategy for photovoltaic emulator using resistance comparison method and binary search method," *Solar Energy*, vol. 153, pp. 83–95, 2017.

[15] J. Gonzalez-Llorente, A. Rambal-Vecino, L. A. Garcia-Rodriguez, J. C. Balda, and E. I. Ortiz-Rivera, "Simple and efficient low power photovoltaic emulator for evaluation of power conditioning systems," in *2016 IEEE Applied Power Electronics Conference and Exposition (APEC)*, pp. 3712–3716, Long Beach, CA, USA, 2016.

[16] Y. Li, T. Lee, F. Z. Peng, and D. Liu, "A hybrid control strategy for photovoltaic simulator," in *2009 Twenty-Fourth Annual IEEE Applied Power Electronics Conference and Exposition*, pp. 899–903, Washington, DC, USA, 2009.